

Heterologous expression, functional characterization and localization of two isoforms of the monkey iron transporter Nramp2

Li ZHANG*, Timothy LEE*, Yue WANG† and Tuck W. SOONG†¹

*Department of Surgery, National University of Singapore, S(119260), Singapore, and †Institute of Molecular and Cell Biology, 30 Medical Drive, S(117609), Singapore

Natural resistance-associated macrophage protein 2 (Nramp2) has been suggested to be involved in transferrin-independent iron uptake. Two isoforms of the Nramp2 gene generated by alternative splicing of the 3' exons were identified in mouse, rat and human, but it is unclear if they perform distinct functions. To rationalize our previous work, which indicated an increase in iron deposition in a Parkinsonian monkey brain, two monkey Nramp2 isoforms were isolated for a comparative study to assess their relative iron-uptake abilities, tissue distribution and subcellular localization. The monkey Nramp2 isoforms, 2a and 2b, exhibit approx. 98% identity at the amino acid level when compared with the human homologues. The Nramp2a transcript contains a canonical iron-responsive element (IRE), whereas that of Nramp2b lacks the IRE motif in the 3' untranslated

region. By reverse transcriptase (RT)-PCR, the mRNAs of both isoforms were detected in all tissues examined. The amino acid differences at the C-terminus neither affected the protein expression levels in HEK-293T and COS-7 cells nor altered the subcellular localization and tissue distribution of the isoforms. Similar levels of iron uptake were detected in the HEK-293T cells transfected with either the Nramp2a or 2b gene, and a reduction of iron from the ferric (Fe³⁺) to the ferrous (Fe²⁺) state is necessary before transport can take place. However, this transferrin-independent uptake of iron into the cells is not a Ca²⁺-dependent process.

Key words: alternative splicing, gene cloning, Parkinson's disease, transferrin-independent iron uptake.

INTRODUCTION

Iron is an essential trace element that is important for many biological processes, including oxygen transport and electron transport during cellular respiration [1,2]. Iron is also important as a cofactor for enzymes involved in neurotransmitter synthesis [3,4]. Overload of free iron has been implicated in the generation of reactive oxygen species, which mediate permanent cell and tissue damage [5–7]. An increased iron concentration was found at the substantia nigra pars compacta (SNPc) in Parkinsonian brains, and it has been suggested that the iron-catalysed production of hydroxyl free radicals might be involved in the onset of the disease [8–11]. We and others have demonstrated that the levels of transferrin or its receptor did not increase in the 1-methyl-4-phenyl-1,2,3,6-tetrahydropyridine (MPTP)- or 6-hydroxydopamine (6-OHDA)-induced Parkinsonian brain, indicating that the transferrin-dependent pathway might not be responsible for the increased influx of iron into the cells [8,12]. Thus the greater iron deposition in neurons and/or glial cells in the SNPc of the Parkinsonian brain might occur by a different iron transport mechanism.

A novel non-haem iron transporter gene was identified in *mk/mk* mouse (Nramp2) by positional cloning [13] and in rat DCT1 (divalent cation transporter 1) by expression cloning in oocytes [7]. DCT1 has been shown to be a membrane-potential-dependent, proton-coupled metal-ion transporter that has a broad range of substrates, including Fe²⁺, Zn²⁺, Mn²⁺, Co²⁺,

Cd²⁺, Cu²⁺, Ni²⁺ and Pb²⁺ [7]. By functional complementation of a *smf1* mutant yeast defective in bivalent cation transport, the mouse Nramp2 transporter was also shown to be capable of Mn²⁺ transport [14]. Heterologous expression of mouse Nramp2 in HEK-293T cells demonstrated that the Nramp2 isoform could functionally transport Fe²⁺ as well. Introduction of the mutation Gly¹⁸⁵ → Arg into the protein abrogated iron-transport activity [15]. This same mutation was discovered both in the microcytic anaemia (mk) mice and in Belgrade (b)-rats, and these animals were also found to be defective in transferrin-mediated iron transport, resulting in severe iron-deficiency anaemia [13,16,17]. These previous studies seem to imply that Nramp2 could be involved in both transferrin-dependent and transferrin-independent transport of iron into the cell. There have also been some contradictory reports regarding the necessity for both a reduction of iron from the ferric to ferrous form and the presence of Ca²⁺ for the transferrin-independent iron-uptake process to occur [18–20]. Clearly, for a better understanding of its roles in iron uptake, the functions and properties of Nramp2 need to be further characterized.

Two Nramp2 isoforms, arising possibly from the alternative use of the polyadenylation signal exons, have been identified in mouse [21], rat [7] and human [22,23]. The spliced mRNA for Nramp2a, but not 2b, contains in its 3' untranslated region a copy of the iron-responsive element (IRE) known to confer iron-dependent stability to the mRNA [24]. The two isoforms have different C-termini. However, whether the two isoforms perform

Abbreviations used: BPS, bathophenanthroline disulphonate; DMEM, Dulbecco's modified Eagle's medium; IRE, iron-responsive element; MPTP, 1-methyl-4-phenyl-1,2,3,6-tetrahydropyridine; Nramp2, natural resistance-associated macrophage protein 2; NTA, nitrilotriacetic acid; 6-OHDA, 6-hydroxydopamine; RT, reverse transcriptase; SNPc, substantia nigra pars compacta; UTR, untranslated region.

¹ To whom correspondence should be addressed, at the present address: National Neuroscience Institute, Irrawaddy Block, 11 Jalan Tan Tock Seng, S(308433), Singapore (e-mail soongtw@yahoo.com).

The nucleotide sequences for the monkey iron transporters Nramp2a and Nramp2b have been deposited in the GenBank® database under GenBank® accession numbers AF153279 and AF153280 respectively.

distinct functions is not known, because the characterization of the functions, localization and regulation of these two isoforms have not been studied in tandem.

Recently, we detected an increase in iron in the SNPc of a MPTP-induced Parkinsonian monkey by nuclear microscopy (Y. He, P.-S. Thong, T. Lee, S.-K. Leong and F. Watt, unpublished work). Meanwhile, Nramp2 mRNA was found to be expressed at a relatively high level in rat SNPc [7]. As an initial step to determine whether Nramp2 is responsible for the increased iron deposition in Parkinsonian monkey brain, we have isolated cDNAs encoding monkey Nramp2a and Nramp2b, and have carried out a comparative study of the two Nramp2 isoforms. Here, we report the characterization of the function and sub-cellular localization of the monkey Nramp2a and Nramp2b in transfected HEK-293T and COS-7 cells, and their distribution in various monkey tissues.

EXPERIMENTAL

Cloning of monkey Nramp2a and Nramp2b cDNA

Monkey Nramp2a and Nramp2b full-length cDNAs were isolated by reverse transcriptase (RT)-PCR. The primers used were obtained from the highly conserved sequences of the 5' and 3' untranslated regions (UTRs) of the Nramp2 genes of the mouse [16,21], rat [7,16] and human [22,23]. The reverse primer for Nramp2a contains an invariant sequence, Mon2aR (5' AAA CAC ACT GGC TCT GAT GGC 3'), which includes the IRE. For Nramp2b, the reverse primer was slightly degenerate, and was designated Mon2bR (5' GAA CAA RYT CAC CTC IGA ACT AA 3'; I = deoxyinosine). A common forward primer MonF1 (5' CT CAG GTA TCC ACC ATG GTG 3') was used for both Nramp2a and Nramp2b (Figure 1). First, the cDNA strand was synthesized by using 1 µg of monkey kidney total RNA and the SUPERScript™ II RT (Gibco BRL, Gaithersburg, MD, U.S.A.). High-fidelity PCR reactions were ensured by using 'hot-start' and a mixture of *Platinum Taq* (Gibco BRL) and *Pfu* (Stratagene, La Jolla, CA, U.S.A.) DNA polymerases in a ratio of 12.5:1. The PCR program was as follows: an initial denaturation was set up at 94 °C for 4 min, followed by 30 cycles of amplification at 94 °C for 40 s, 50 °C for 1 min, 72 °C for 2 min, and a final extension at 72 °C for 10 min. The PCR products were cloned into a pGEMTeasy vector (Promega, Madison, WI, U.S.A.), and sequenced using an ABI model 377 Automated DNA Sequencer (Perkin-Elmer, Norwalk, CT, U.S.A.).

Southern blot analysis of genomic DNA

Southern blotting for Nramp2 was performed following standard protocols [25]. The blot was hybridized to a 321-bp ³²P-labelled Nramp2 probe (nt 862 to 1182) at 60 °C for 16 h, and washed at 60 °C in 0.2 × SSC/0.1 % SDS (where 1 × SSC is 0.15 M NaCl/0.015 M sodium citrate).

Hemi-nested RT-PCR for detecting tissue distribution of monkey Nramp2 mRNA

Total RNA was isolated by using TRIZOL™ Reagent (Gibco BRL) from frozen tissues of adult male monkeys (*Macaca fascicularis*): cerebral cortex, cerebellum, medulla, lung, liver, spleen, kidney, testis and skeletal muscle. Of each RNA, 1 µg was used for RT-PCR. In the first round of amplification, the forward primer MonF3 (5' TGT ACC TGC ATT CTG CCT TAG 3') was used for both Nramp2a and Nramp2b. The reverse primer for Nramp2a was 2aProbe (5' ATC CAG TGT TAT TTA GTG TAG 3'), and the reverse primer for Nramp2b was

2bProbe (5' AAC TAA CAG AGA TGT TAA CAG 3'). The resulting PCR products were gel-purified (Qiagen, Hilden, Germany) and 1 µl of the eluted PCR products from different tissues were used as templates for secondary PCR reactions. The forward primer for both Nramp2a and Nramp2b was changed to HybriF (5' GAA GTT CGA GAA GCC AAT AAG 3'), which was 56 bp downstream of MonF3. The reaction mixture lacking RT was used as a negative control in the RT-PCR procedure; reaction mixture without cDNA was used as a negative control in secondary PCR. The cloned Nramp2a and Nramp2b cDNAs were used as templates for testing the specificity of the PCR amplifications.

Construction of Nramp2-c-Myc expression plasmids

The Kozak sequences (CCACC) [26] were introduced by PCR immediately upstream of the ATG start codon of Nramp2a or Nramp2b, while sequences encoding three tandem copies of the c-Myc antigenic peptide (GEQKLISEEDLN) were ligated in-frame at the 3' end. The Nramp2-c-Myc sequences were then subcloned into the eukaryotic expression vector, pRc/RSV (Invitrogen, Carlsbad, CA, U.S.A.).

Cell culture and transient transfection

COS-7 and HEK-293T cells were maintained in Dulbecco's modified Eagle's medium (DMEM) supplemented with 10 % (v/v) fetal-bovine serum, 2 mM L-glutamine, 100 units/ml penicillin, 100 µg/ml streptomycin and 0.25 µg/ml amphotericin B. These cells were grown to a density of 2 × 10⁵ in six-well Nunclon™ dishes for Western blotting, or on poly-(D-lysine)-treated cover slides for immunostaining. For iron-uptake assay, the cells were grown in 9-cm Nunclon™ dishes to a density of 2 × 10⁶. Expression plasmid (0.2 µg or 1 µg) was added to each well for transfection by using the Qiagen Effectene Transfection Kit, as described by the manufacturer. For negative controls, the cells were transfected either with vector alone or without DNA.

Western blotting and immunocytochemistry

After transfection (48 h), the cells grown in six-well dishes were trypsin-treated and collected. The cells were then resuspended in 300 µl of cell-disruption buffer [0.2 M Tris/HCl, 10 mM MgCl₂, 1 mM dithiothreitol, 10 % (v/v) glycerol, 2 mM PMSF and 2 µg/ml pepstatin A (pH 8.0)], and sonicated. The homogenates were centrifuged and proteins in the supernatant were collected. Upon determination of the concentration by Bradford assay, 10 µg of protein from the supernatant was loaded on to an SDS/10 %-polyacrylamide gel, and electrophoresed (SDS/PAGE) under reducing conditions. Following gel electrophoresis, the fractionated proteins were transferred in blotting buffer [20 % (v/v) methanol, 25 mM Tris base, 192 mM glycine and 0.1 % (w/v) SDS] to Hybond-C extra membrane (Amersham, Piscataway, NJ, U.S.A.) overnight at 4 °C. The blot was blocked for 1 h with PBS containing 5 % (w/v) skimmed milk and 0.1 % (v/v) Triton X-100, washed, and incubated for 2 h with an anti-(c-Myc) antibody (9E10; Santa Cruz Biotechnology Santa Cruz, CA, U.S.A.) diluted 1:1000. The membranes were washed three times in 0.1 % Triton X-100 in PBS, incubated for 1 h with horseradish-peroxidase-conjugated anti-mouse IgG (Pierce, Rockford, IL, U.S.A.) diluted 1:8000, and washed three times in 0.1 % Triton X-100 in PBS. Proteins were revealed using enhanced chemiluminescence lighting system (ECL; Pierce). To detect actin protein, the membrane was reprobed with a monoclonal antibody raised against actin (Boehringer Mannheim, Mannheim, Germany) diluted 1:500.

For immunostaining, 48 h after transfection the cells growing on cover slips were washed with PBS and fixed with 3.7% (w/v) paraformaldehyde for 10 min. After blocking with 10% (v/v) normal sheep serum for 10 min, the cells were incubated with the anti-(c-Myc) antibody (9E10) diluted 1:1000 overnight at 4 °C. The cells were then washed three times in 0.1% Triton X-100 in PBS, and incubated for 1 h with fluorescein-conjugated sheep anti-mouse IgG (Boehringer Mannheim) diluted to 20 µg/ml. This was followed by three changes of PBS to remove unreacted secondary antibody. The cells were then counterstained with propidium iodide and viewed under a Zeiss confocal microscope.

Transferrin-independent iron-uptake assay

⁵⁵Fe-nitrilotriacetic acid (⁵⁵Fe-NTA) was prepared by addition of ⁵⁵FeCl₃ (New England Nuclear, Beverly, MA, U.S.A.) to a 20-fold molar excess of the disodium salt of NTA. After transfection (48 h), the cells growing in 9-cm dishes were incubated for 1 h in serum-free DMEM to deplete cells of transferrin. The cells were then washed with PBS and washing buffer (25 mM Tris, 25 mM Mes, 140 mM NaCl, 5.4 mM KCl, 5 mM glucose, 1.8 mM CaCl₂ and 800 µM MgSO₄, pH 5.5) before incubation in a buffer (25 mM Tris, 25 mM Mes, 140 mM NaCl, 5.4 mM KCl, 5 mM glucose, 1.8 mM CaCl₂ and 800 µM MgSO₄, pH 5.5) containing 1 µM ⁵⁵Fe-NTA at 37 °C for 20 min. For ferrous iron-uptake assay, 50 µM ascorbic acid was added in the incubation buffer to keep the iron in the ferrous state. The cells were then washed with incubation buffer and removed by digestion with 2 ml of 0.5% trypsin/EDTA (Sigma, St. Louis, MO, U.S.A.) at 37 °C for 2 min. Cells were washed with ice-cold washing buffer and centrifuged twice. The cell pellet was dissolved in 1 ml of liquid-scintillation cocktail (ICN Biomedicals, Costa Mesa, CA, U.S.A.). Radioactivity was determined by using a Beckman LS6000 scintillation counter with a band-width of 0 to 400.

To determine whether the reduction of ferric iron is required for transport via Nramp2, the impermeable ferrous iron chelator, bathophenanthroline disulphonate (BPS), was used. After transfection (24 h), the cells grown in 9-cm dishes were split equally into four wells of the six-well multidishes pretreated with poly-(D-lysine). The cells were then cultured for a further 24 h in an air/CO₂ mixture (19:1) at 37 °C. Ferric iron-uptake assay was performed as described above, except that BPS was added in the incubation buffer. Toxicity assays of BPS on the cells were performed similarly, except that the cells were put back into culture to assess viability after exposure to various concentrations of BPS up to 10 µM. All the experiments were repeated three times.

To investigate the effects of Ca²⁺ on the function of Nramp2, cells were split and grown on poly-(D-lysine)-treated dishes 24 h after transfection. After transfection (48 h), the cells were incubated in serum-free DMEM for 1 h, and washed with PBS. The cells were then washed twice in 1 mM EGTA for 5 min. Ferrous iron uptake was measured as above, except that Ca²⁺ was removed from the washing buffer and added to the incubation buffer at various concentrations. The time for iron uptake was reduced from 20 to 10 min. The cells not washed in EGTA were used as a control; once again, three independent experiments were performed.

RESULTS

Isolation of cDNAs encoding the two isoforms of monkey Nramp2

By designing degenerate oligonucleotides that correspond to conserved regions of the Nramp2 proteins, we were able to

isolate a partial cDNA from monkey-kidney and -brain mRNAs. Alignment of this monkey partial Nramp2 cDNA sequence with the mouse, rat and human DNA sequences revealed a very high homology with the Nramp2 DNA sequences among the different species (results not shown). Subsequent alignment of the DNA sequences of the 5' and 3' UTRs flanking the various Nramp-2a and -2b genes from mouse, rat and human helped in the design of the PCR primers for the cloning of the complete coding sequences for the two isoforms of the monkey Nramp2 genes by the RT-PCR method (Figure 1). The high fidelity in RT-PCR cloning was demonstrated by the identical sequences of six Nramp2a and seven Nramp2b clones analysed. The monkey Nramp-2a and -2b sequences have been deposited into GenBank® (accession numbers AF153279 and AF153280 respectively) and the only difference between the two isoforms is found in the C-terminus, in which there are also an extra 7 amino acids in Nramp2b (Figure 2). Both isoforms display approx. 91% to approx. 98% identity at the amino acid level with the mouse, rat and human Nramp2 proteins. The Kyte-Doolittle hydrophilicity

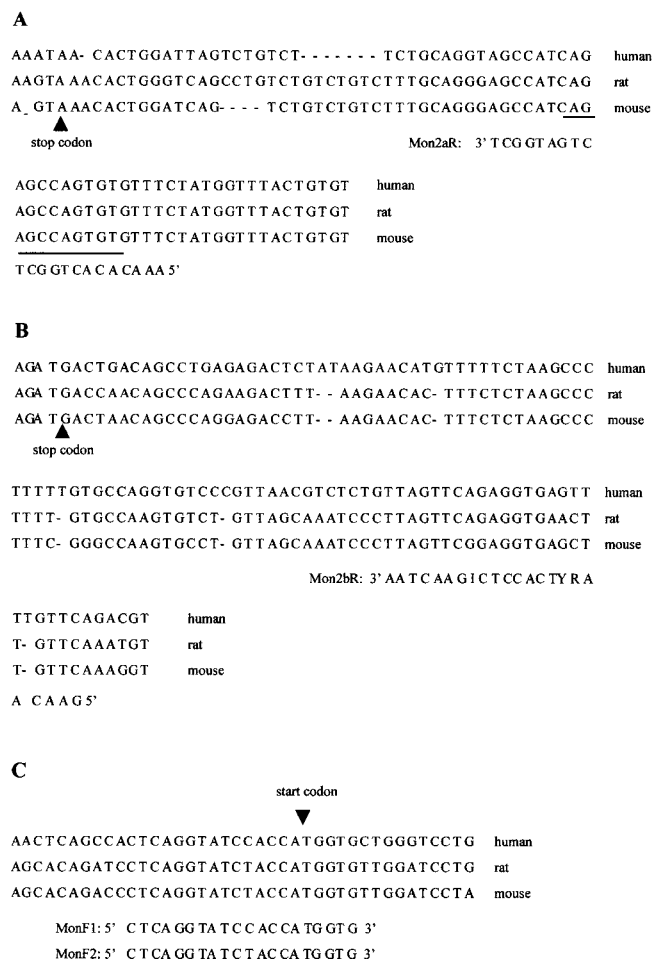


Figure 1 Primers for cloning of monkey Nramp2a and Nramp2b cDNA

(A) The reverse primer Mon2aR was chosen by comparing the 3' UTRs of human, rat and mouse Nramp2a transcripts. The conserved IREs are underlined. The nucleotide sequence for Mon2aR is shown under the alignment. (B) The reverse primer Mon2bR was designed to target a conserved sequence in the 3' UTRs of Nramp2b transcripts. The nucleotide sequence of this primer is slightly degenerate, and is shown under the alignment. I, deoxyinosine. (C) Two forward primers, MonF1 and MonF2, were designed by comparing sequences across the start codon. There was only a single base difference between MonF1 and MonF2.

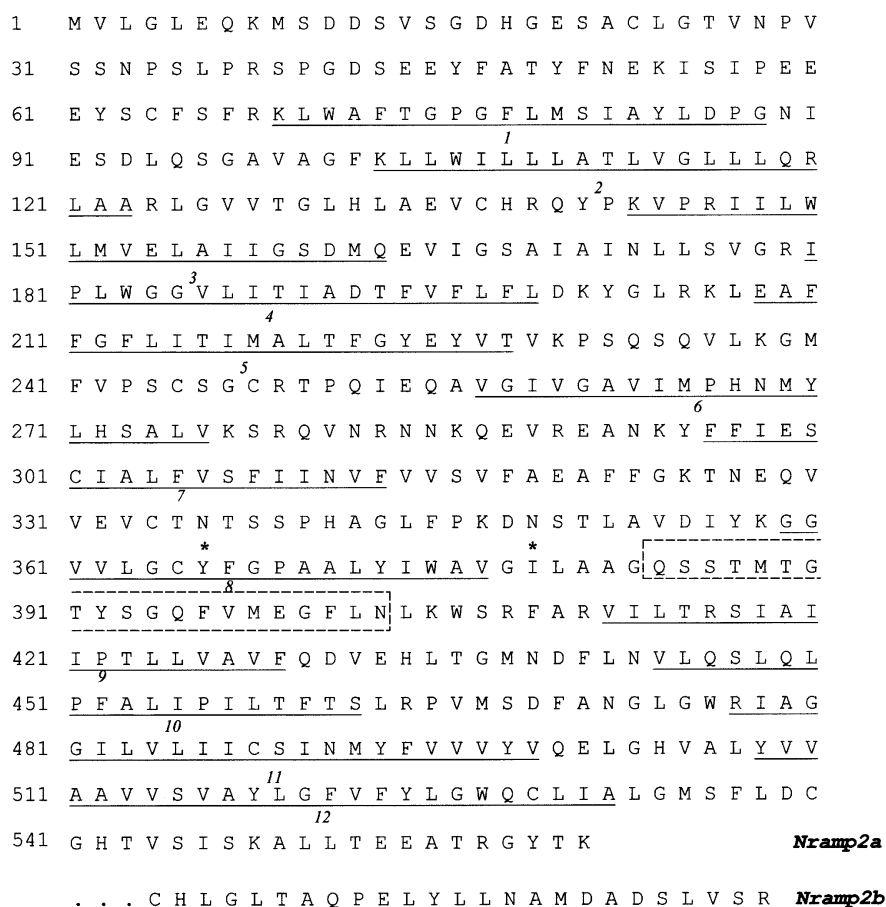


Figure 2 The deduced amino acids of the monkey Nramp2a protein

The 12 putative transmembrane regions are indicated by horizontal bars; the consensus transport motif is boxed by dashed lines. Two predicted N-linked glycosylation sites are indicated by the asterisks (*). The monkey Nramp2b protein only differs from Nramp2a in the C-terminus.

plot predicts that the monkey Nramp2 protein should contain 12 transmembrane domains with both N- and C-termini projecting into the cytoplasm. The monkey Nramp2 protein contains the common prokaryotic and eukaryotic transporter motif (amino acids 384–403) known as the ‘binding-protein-dependent, inner-membrane-component transport signature’ [27]. Between transmembrane segments 7 and 8 is a large predicted extracellular loop that contains two putative glycosylation sites. Southern blot analysis detected a single band from monkey genomic DNA digested with various restriction enzymes (results not shown), indicating that Nramp2 is a single gene.

Tissue distribution of monkey Nramp2a and Nramp2b mRNA

Previous studies have shown that the expression of mouse Nramp1 is restricted to the macrophages, whereas the mouse, rat and human Nramp2 genes are expressed ubiquitously in many tissues and cell types [7,21,28]. To date, the tissue distributions of Nramp-2a and -2b have not been compared. To determine if Nramp-2a and -2b are differentially expressed in different tissues, or if there are cellular mechanisms that preferentially generate one splice form over the other, we used the RT-PCR technique to examine the expression patterns of the mRNAs for the two isoforms (Figure 3). The PCR conditions were optimized for specific amplification of each isoform. The negative control, in

which no RT was added, did not yield any PCR product. The specific PCR products for both Nramp2a and Nramp2b were detected from the total RNA prepared from all the tissues examined. The aggregate levels of Nramp-2a and -2b mRNAs were uneven among different tissues. The mRNA levels in brain, kidney, testis, liver and skeletal muscle were comparable, but higher than those in lung and spleen.

Subcellular localization of Nramp-2a and -2b

We made two expression constructs where a DNA sequence encoding three tandem copies of c-Myc epitope was fused in frame to the C-terminal end of Nramp2a- and Nramp2b-coding regions. The c-Myc-tagged Nramp2 proteins were expressed in transfected cells, and their cellular localization was determined by immunostaining using an anti-(c-Myc) antibody. After transfection, the transient expression of the Nramp2 proteins was first examined by Western blot analysis (Figure 4A). A major band of approx. 65 kDa, close to the predicted molecular mass of the Nramp2 proteins, was produced in the HEK-293T cells transfected with either Nramp2a (Figure 4A, lane 3) or Nramp2b (Figure 4A, lane 4) gene. Faint bands of approx. 90 kDa were also observed, which were probably the glycosylated forms of the Nramp2 proteins. No band was detected in the extracts of

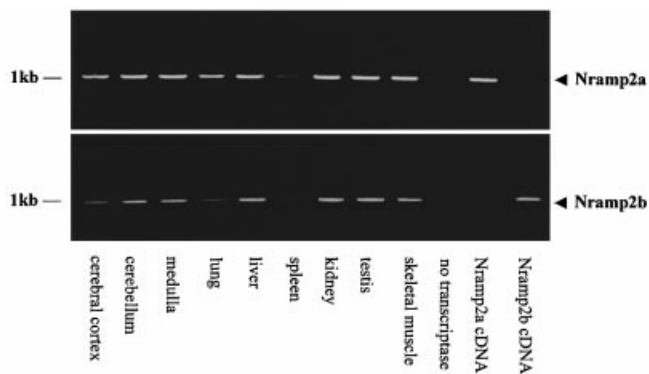


Figure 3 Hemi-nested RT-PCR for detecting tissue distribution of the two isoforms of the monkey Nramp2 gene

Total RNA (1 μ g) from different monkey tissues was used. For a negative control, no RT was added. Cloned cDNA for Nramp2a or Nramp2b was also used as a control in PCR reactions.

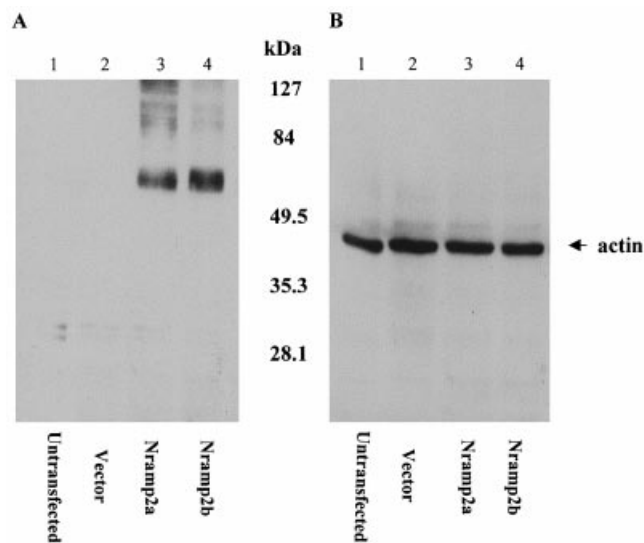


Figure 4 Western blot analysis of Nramp2 expression in HEK-293T cells transfected with c-Myc-tagged Nramp2a or Nramp2b

Each lane contains 10 μ g of proteins. The blot was first probed with monoclonal anti-(c-Myc) antibody (A), and then reprobed with anti-actin antibody (B). Lanes 1, untransfected cells; lanes 2, cells transfected with pRC/RSV vector alone; lanes 3, cells transfected with Nramp2a construct; lanes 4, cells transfected with Nramp2b construct.

the untransfected cells or cells transfected with the expression vector alone. Each lane was also stained for actin to demonstrate that similar amounts of protein were used (Figure 4B).

The subcellular localization of the two Nramp2 isoforms was determined by immunostaining using c-Myc antibody. Confocal microscopy demonstrated that the localization patterns of Nramp-2a and -2b proteins were similar. Both isoforms showed strong punctate staining in the cytoplasm, and a faint staining on the plasma membrane (Figures 5C, 5D, 5G and 5H). This pattern was observed in both the COS-7 (Figure 5C and 5D) and HEK-293T (Figures 5G and 5H) cells transfected with constructs for both isoforms. Untransfected cells (Figures 5A and 5E) or cells transfected with the vector alone (Figures 5B and 5F) exhibited only propidium iodide staining for the nucleus, with no

fluorescein signals at all. The punctate staining pattern suggests an endosomal localization of the Nramp2 proteins, which has also been demonstrated in other studies describing Nramp2 colocalization with transferrin receptors in endosomes and its presence in the endosomal membrane fraction [15,17]. The results above demonstrate that the different C-termini affected neither the expression levels of the two Nramp2 isoforms nor their subcellular localization in the transfected cells.

Monkey Nramp2a and Nramp2b demonstrate a similar ability in the transferrin-independent uptake of iron

The ability of Nramp2a and Nramp2b in iron transport has not been compared. Our Western blotting results above revealed similar levels of protein expression for both Nramp2 isoforms in transiently transfected HEK-293T or COS-7 cells. To determine whether the difference in the C-termini might play a regulatory role in the protein's iron transport activity, we carried out assays to measure the uptake of $^{55}\text{Fe}^{2+}$ or $^{55}\text{Fe}^{3+}$ by HEK-293T cells transfected with either Nramp2a or Nramp2b construct. Both Nramp2a and Nramp2b were found to confer on the transfected cells the same level of iron transport, giving rise to more than a 150-fold increase of $^{55}\text{Fe}^{2+}$ uptake and a 50-fold increase of $^{55}\text{Fe}^{3+}$ uptake over untransfected or vector-transfected HEK-293T cells (Figures 6A and 6B). This result shows that the difference in the C-termini again has no detectable effect on the iron-transport efficiency of the two monkey Nramp2 isoforms, at least under the experimental conditions used. However, it should be noted that, in the overexpression system, the total effect will be largely amplified. This might be the reason why there is such a marked increase in the cross-plasma-membrane ^{55}Fe uptake via Nramp2, although most of the protein is localized in endosomes in the transfected cells. In order to investigate transferrin-independent iron transport via Nramp2 expressed on the plasma membrane, we minimized the possible contamination by transferrin in our experiments. This was done by incubating the transfected cells first in serum-free medium to deplete transferrin and at pH 5.5, a pH value at which transferrin binds iron poorly and is not internalized by the cells [18]. The stronger Nramp2 expression on the endosomal membrane (Figure 5) might result in an even higher level of iron uptake via the transferrin-dependent pathway.

Fe^{3+} reduction is a prerequisite of iron transport by monkey Nramp2

Iron uptake by Nramp2 decreased greatly (by approx. 14-fold) in transfected HEK-293T cells when $^{55}\text{Fe}^{2+}$ -NTA was replaced with $^{55}\text{Fe}^{3+}$ -NTA. However, iron uptake in these cells was still much higher than that of untransfected cells (Figure 6B). The higher uptake rate of Fe^{2+} over Fe^{3+} raises the question of whether Nramp2p transports Fe^{2+} more efficiently, or a reduction of Fe^{3+} to Fe^{2+} is a prerequisite for transport to happen. We addressed this question by using different concentrations of BPS, a selective impermeant Fe^{2+} chelator, to block ferrous-iron transport by Nramp2p. A decrease of Fe^{3+} transport was observed with the increase in BPS concentration. At 1 μM BPS, approx. 75% of iron uptake was inhibited and, in the presence of 10 μM BPS, Fe^{3+} transport was reduced to near-background level (Figure 7). Similar results were also obtained when another ferrous iron chelator, ferrozine, was used (results not shown). This result indicates that a reduction of Fe^{3+} to Fe^{2+} is necessary before iron uptake by Nramp2 proteins occurs.

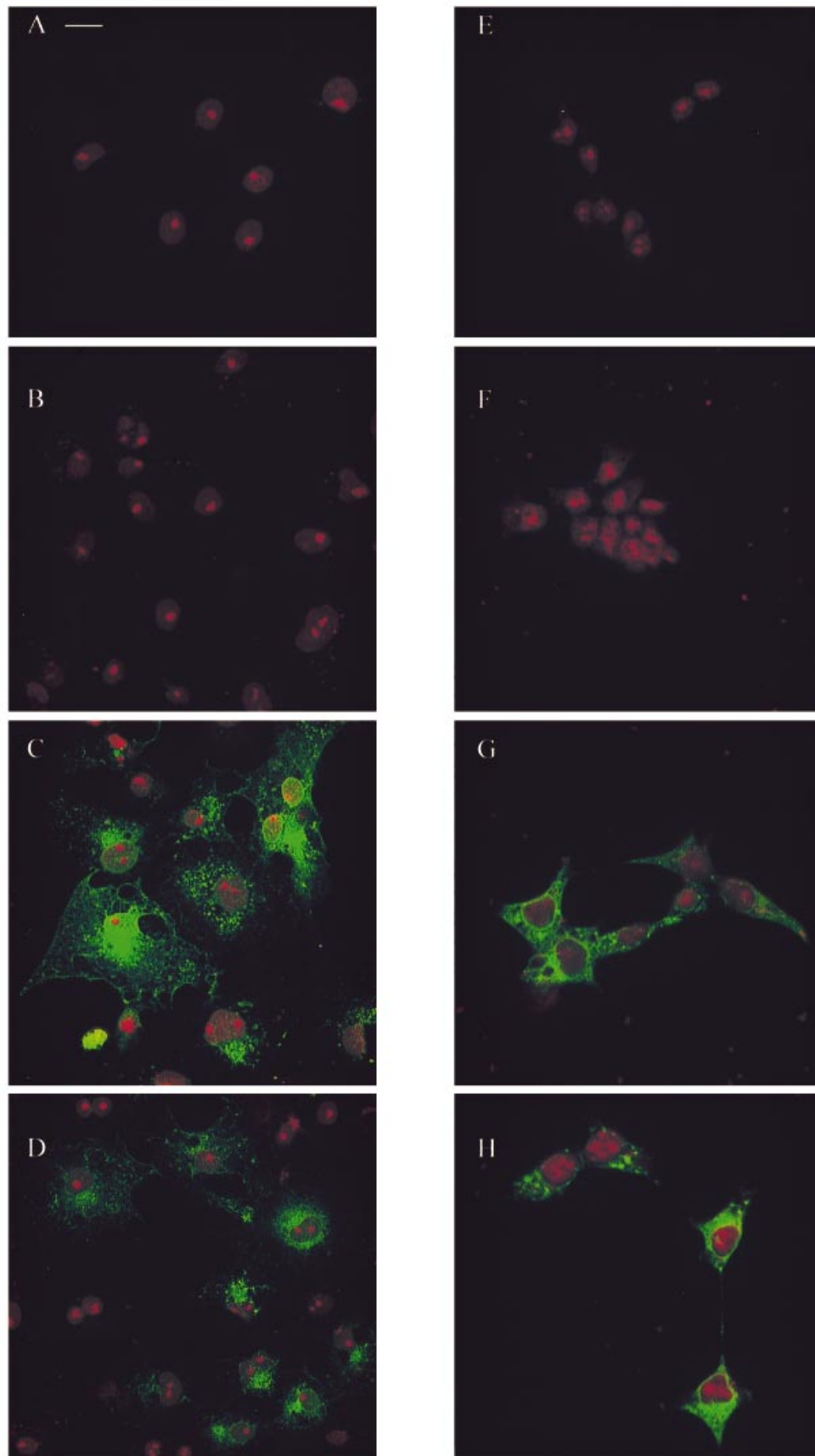


Figure 5 For legend see facing page.

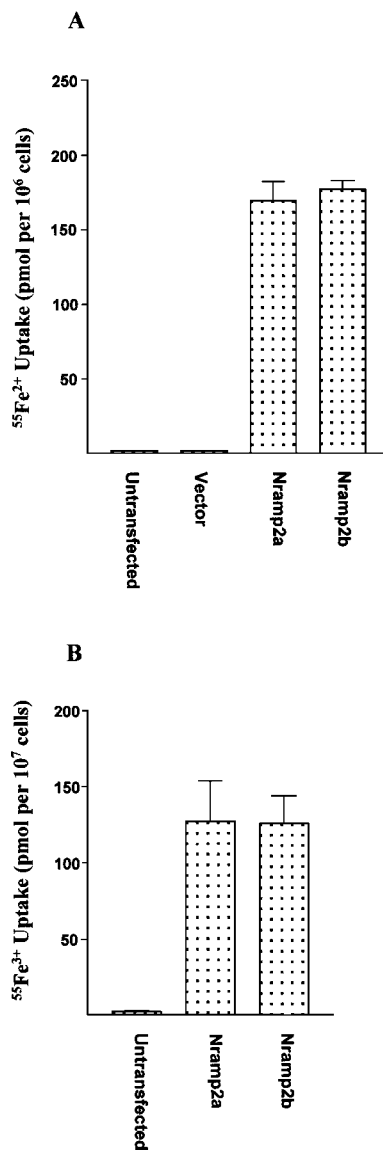


Figure 6 Iron transport activity of Nramp2a and Nramp2b

Non-transfected HEK-293T cells and cells transfected with the constructs indicated were incubated for 20 min in incubation buffer containing $1 \mu\text{M}$ $^{55}\text{Fe}^{2+}$ -NTA (A) or $^{55}\text{Fe}^{3+}$ -NTA (B). The radioactivity was then determined.

Iron uptake of Nramp2 is not Ca^{2+} -dependent

Transferrin-independent iron uptake has been shown to be Ca^{2+} -dependent in most cells [20]. To determine whether Ca^{2+} has a role in regulating the iron transport by Nramp2 protein, we examined the effect of Ca^{2+} in the iron-transport process in Nramp2-transfected HEK-293T cells. Iron-uptake assay conducted in Ca^{2+} -free buffer did not show a decrease in $^{55}\text{Fe}^{2+}$ -NTA transport. Instead, when 10 mM Ca^{2+} was used, iron

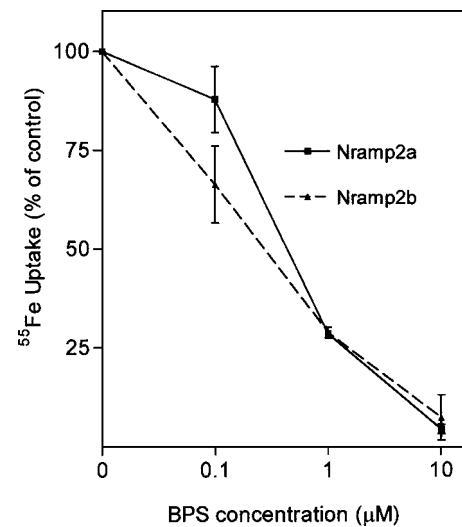


Figure 7 Effect of BPS on Fe^{2+} and Fe^{3+} uptake mediated by Nramp2 expressed in HEK-293T cells

Non-transfected HEK-293T cells and cells transfected with constructs indicated were incubated for 20 min in incubation buffer with $1 \mu\text{M}$ $^{55}\text{Fe}^{3+}$ -NTA and different concentrations of BPS. The radioactivity was then determined. Iron uptake in non-transfected cells was taken as the background level, and subtracted from that of transfected cells. The amount of uptake determined in the absence of BPS was defined as 100%.

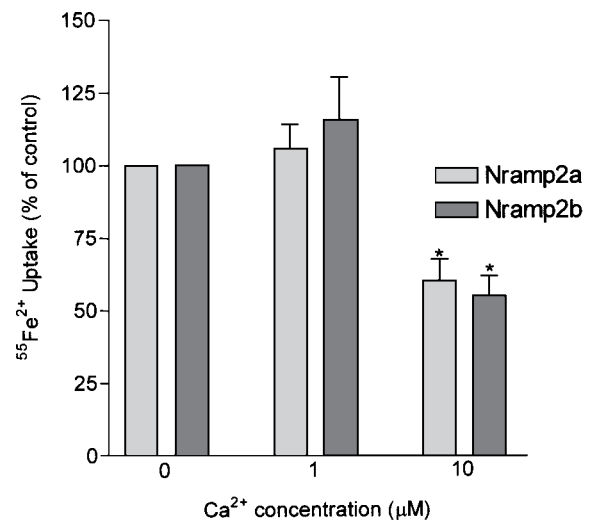


Figure 8 Effect of Ca^{2+} on iron-transport activity of Nramp2

Non-transfected cells and transfected HEK-293T cells were treated with EGTA as described in the Experimental section, and then incubated for 10 min with $^{55}\text{Fe}^{2+}$ -NTA and different concentrations of Ca^{2+} . The iron uptake of non-transfected cells was deducted from that of transfected cells. The amount of radioactivity accumulated in the absence of Ca^{2+} was defined as 100%. *, $P < 0.05$ compared with control, as determined by using the Mann-Whitney test.

Figure 5 Subcellular localization of Nramp2a and Nramp2b proteins

Two cell lines, COS-7 (A–D) and HEK-293T (E–H), were used for this study. Non-transfected cells (A, E) and cells transfected with the vector alone (B, F) serve as negative controls. Both types of cell were transfected with a construct expressing either Nramp2a (C, G) or Nramp2b (D, H). Cells were stained with both the nuclear stain, propidium iodide (red), and anti-(c-Myc) antibody plus fluorescein-conjugated sheep anti-mouse IgG (green). The scale bar shown in (A) represents $20 \mu\text{m}$, and is applicable for B–H.

uptake was decreased by 40% (Figure 8). This result suggests that Ca^{2+} was not required for iron uptake.

DISCUSSION

As a first step towards an understanding of whether Nramp2 is responsible for iron accumulation in the SNPs in a Parkinsonian monkey brain, we isolated cDNAs for the two isoforms of monkey Nramp2. The study of Nramp2a of other mammalian species has been reported, with a cursory mention about the Nramp2b protein [7,16,23]. In the present study we report a comparative analysis of the functional characteristics and localization of the two monkey iron-transporter isoforms. The monkey Nramp2 proteins show the highest amino acid identity, of approx. 98% with their human counterparts. The extremely high identity at the DNA level enabled the cloning of the complete open reading frames of the two monkey Nramp2 isoforms by RT-PCR.

Similar to the mouse and human homologues, the monkey Nramp2 gene is a single gene. It is possible that, like its counterparts, the two monkey isoforms were generated by alternative splicing of Nramp2 transcripts. The physiological significance of these two isoforms is unknown. Our attempts to address this question showed that first, the two isoforms were present ubiquitously in all the monkey tissues examined, with a putative difference in the level of expression in the cerebral cortex, lung and spleen. *In-situ*-hybridization analysis might give a better semi-quantitative measurement of the relative amounts of the two isoforms in a cell type. Secondly, the different C-termini do not seem to have any effect on the subcellular localization, the level of protein expression or iron uptake in either COS-7 or HEK-293T cells.

Previous studies showed that mouse, rat and human Nramp2 proteins could be involved in transferrin-independent iron uptake [7,15]. Our results showed that both Nramp-2a and -2b could be expressed in human HEK-293T cells to induce robust uptake of ^{55}Fe into the transfected cells via a transferrin-independent pathway. The levels of transport for both proteins were comparable, which again points towards their functional similarities, in spite of the differences in the carboxy tails.

Previous studies have not shown whether Nramp2 was able to transport Fe^{3+} [7,15]. Here, we have demonstrated by using a specific ferrous chelator, BPS, that the iron uptake by monkey Nramp2 requires the reduction of Fe^{3+} to Fe^{2+} . The dosage and time of BPS treatment were found not to be toxic to the cells (results not shown), and therefore the reduced iron uptake in the presence of BPS reflects not only the unavailability of Fe^{2+} , but also the inability of Nramp2 to transport Fe^{3+} . The effect of BPS and the higher uptake rate of Fe^{2+} over Fe^{3+} both demonstrated the requirement for the reduction of Fe^{3+} to Fe^{2+} before transport mediated by Nramp2 occurred.

In many types of cells, transferrin-independent iron uptake is Ca^{2+} -dependent [20]. Consistent with the results of Gunshin et al. [7], we have shown that, in the presence of Ca^{2+} , iron uptake was not induced, but instead, at 10 mM concentration, inhibition of transport was observed. The Ca^{2+} -independent iron transport by the monkey Nramp2p suggests that there might be other iron transporters in those cells that showed a Ca^{2+} -dependence in the transferrin-independent iron-transport processes. Previous studies also showed that low-affinity, transferrin-independent iron transport in rat erythroid cells demonstrates little dependence on Nramp2 (DMT1) [29]. These studies, together with our observations, suggest that transferrin-independent iron transport in mammalian cells is mediated probably by multiple pathways via different transport proteins.

Taken together, our results have shown that Nramp2a and Nramp2b have very similar functional characteristics. The major difference in function of the Nramp2 isoforms could lie in their post-transcriptional regulation. Nramp2a contains the IRE sequence and, in mouse and rat, animals fed on iron-deficient diets showed a marked increase in Nramp2a mRNA expression levels [30]. Our attempts to study post-transcriptional regulation by iron in COS-7 cells exposed to high external iron concentrations did not detect an obvious decrease in Nramp2a mRNA level by specific RT-PCR. One possibility is that the amount of intracellular iron loaded via the transferrin-independent pathway was insufficient to generate a detectable difference in mRNA levels of the two isoforms. However, neither supplying cells with transferrin nor overexpressing the 3'UTR-truncated Nramp-2a and -2b clones in COS-7 cells produced any difference in the expression patterns of the Nramp-2a and -2b mRNAs (results not shown). Another possibility is that COS-7 cells might not contain the IRE-binding protein that is essential to stabilize the Nramp2a mRNA. To address further the question of the physiological role of the two isoforms, work is still in progress to identify the localization *in situ* of both isoforms to determine their extent and levels of expression in each cell type in the brain. The ratio of the expression of the Nramp-2a and -2b mRNAs in a cell might shed light on our understanding of the overall regulation of iron uptake, and the response to either iron deficiency or overload in an animal. Knowledge of the expression levels of the monkey Nramp2 isoforms will help to determine whether the iron deposition in the pathological area of the Parkinsonian monkey brain was due to an increased iron uptake through the Nramp2 iron transporter. Subsequently, the pathophysiological mechanisms that lead to Parkinson disease can be investigated.

This work was supported by a grant, RP3950376, from the National University of Singapore. L. Z. is a recipient of the National University of Singapore scholarship award. We thank Dr Wai-Ho Yap for reading the manuscript critically, Dr Alice Tay for sequencing the Nramp2 clones, Narendrakumar Ramanan for helpful discussions, and Dr Ratha Mahendran and Tan-Fong Yong for able technical assistance.

REFERENCES

- Karlin, K. D. (1993) Metalloenzymes, structural motifs, and inorganic models. *Science* **261**, 701–708
- Aisen, P. (1994) Iron metabolism: an evolutionary perspective. In *Iron Metabolism in Health and Disease* (Brock, J. H., Halliday, J. W., Pippard, M. J. and Powell, L. W., eds.), pp. 1–30. W. B. Saunders, London
- Beard, J. D., Connor, J. R. and Jones, B. C. (1993) Iron in the brain. *Nutr. Rev.* **51**, 157–179
- Roskams, A. J. I. and Connor, J. R. (1994) Iron, transferrin, and ferritin in the rat brain during development and aging. *J. Neurochem.* **63**, 709–716
- Gerlach, M., Ben-Shachar, D., Riederer, P. and Youdim, M. B. H. (1994) Altered brain metabolism of iron as a cause of neurodegenerative diseases? *J. Neurochem.* **63**, 793–807
- Gelman, B. B. (1995) Iron in CNS disease. *J. Neuropathol. Exp. Neurol.* **54**, 477–486
- Gunshin, H., Mackenzie, B., Berger, U. V., Gunshin, Y., Romero, M. F., Boron, W. F., Nussberger, S., Gollan, J. L. and Hediger, M. A. (1997) Cloning and characterization of a mammalian proton-coupled metal-ion transporter. *Nature (London)* **388**, 482–488
- Goto, K., Mochizuki, H., Imai, H., Akiyama, H. and Mizuno, Y. (1996) An immunohistochemical study of ferritin in 1-methyl-4-phenyl-1,2,3,6-tetrahydropyridine (MPTP)-induced hemiparkinsonian monkeys. *Brain Res.* **724**, 125–128
- He, Y., Thong, P. S., Lee, T., Leong, S. K., Shi, C. Y., Wong, P. T., Yuan, S. Y. and Watt, F. (1996) Increased iron in the substantia nigra of 6-OHDA induced parkinsonian rats: a nuclear microscopy study. *Brain Res.* **735**, 149–153
- Jenner, P. and Olanow, C. W. (1996) Oxidative stress and the pathogenesis of Parkinson's disease. *Neurology* **47**, S161–S170
- Qian, Z. M. and Wang, Q. (1998) Expression of iron transport proteins and excessive iron accumulation in the brain in neurodegenerative disorders. *Brain Res. Rev.* **27**, 257–267

- 12 He, Y., Lee, T. and Leong, S. K. (1999) Time-course and localization of transferrin receptor expression in the substantia nigra of 6-hydroxydopamine-induced parkinsonian rats. *Neuroscience* **91**, 579–585
- 13 Fleming, M. D., Trenor, III, C. C., Su, M. A., Foerzler, D., Beier, D. R., Dietrich, W. F. and Andrews, N. C. (1997) Microcytic anaemia mice have a mutation in Nramp2, a candidate iron transporter gene. *Nat. Genet.* **16**, 383–386
- 14 Pinner, E., Gruenheid, S., Raymond, M. and Gros, P. (1997) Functional complementation of the yeast bivalent cation transporter family SMF by NRAMP2, a member of the mammalian natural resistance-associated macrophage protein family. *J. Biol. Chem.* **272**, 28933–28938
- 15 Su, M. A., Trenor, C. C., Fleming, J. C., Fleming, M. D. and Andrews, N. C. (1998) The G185R mutation disrupts function of the iron transporter Nramp2. *Blood* **92**, 2157–2163
- 16 Fleming, M. D., Romano, M. A., Su, M. A., Garrick, L. M., Garrick, M. D. and Andrews, N. C. (1998) Nramp2 is mutated in the anemic Belgrade (b) rat: evidence of a role for Nramp2 in endosomal iron transport. *Proc. Natl. Acad. Sci. U.S.A.* **95**, 1148–1153
- 17 Gruenheid, S., Canonne-Hergaux, F., Gauthier, S., Hackam, D. J., Grinstein, S. and Gros, P. (1999) The iron transporter protein Nramp2 is an integral membrane glycoprotein that colocalizes with transferrin in recycling endosomes. *J. Exp. Med.* **189**, 831–841
- 18 Sturrock, A., Alexander, J., Lamb, J., Craven, C. M. and Kaplan, J. (1990) Characterization of a transferrin-independent uptake system for iron in HeLa cells. *J. Biol. Chem.* **265**, 3139–3145
- 19 Barisani, D., Berg, C. L., Wessling-Resnick, M. and Gollan, J. L. (1995) Evidence for a low K_m transporter for non-transferrin-bound iron in isolated rat hepatocytes. *Am. J. Physiol.* **269**, G570–G576
- 20 de Silva, D. M., Askwith, C. C. and Kaplan, J. (1996) Molecular mechanisms of iron uptake in eukaryotes. *Physiol. Rev.* **76**, 31–47
- 21 Gruenheid, S., Cellier, M., Vidal, S. and Gros, P. (1995) Identification and characterization of a second mouse Nramp gene. *Genomics* **25**, 14–25
- 22 Kishi, F. and Tabuchi, M. (1997) Complete nucleotide sequence of human NRAMP2 cDNA. *Mol. Immunol.* **34**, 839–842
- 23 Lee, P. L., Gelbart, T., West, C., Halloran, C. and Beutler, E. (1998) The human Nramp2 gene: characterization of the gene structure, alternative splicing, promoter region and polymorphisms. *Blood Cells Mol. Dis.* **24**, 199–215
- 24 Casey, J. L., Hentze, M. W., Koeller, D. M., Caughman, S. W., Rouault, T. A., Klausner, R. D. and Harford, J. B. (1988) Iron-responsive elements: regulatory RNA sequences that control mRNA levels and translation. *Science* **240**, 924–928
- 25 Sambrook, J., Fritsch, E. F. and Maniatis, T. (1989) Southern blot in Molecular cloning: a laboratory manual, pp. 11–111, Cold Spring Harbor Laboratory, Cold Spring Harbor, NY
- 26 Kozak, M. (1991) Structural features in eukaryotic mRNAs that modulate the initiation of translation. *J. Biol. Chem.* **266**, 19867–19870
- 27 Bairoch, A. (1991) PROSITE: a dictionary of sites and patterns in proteins. *Nucleic Acids Res.* **19**, 2241–2245
- 28 Kishi, F. and Tabuchi, M. (1998) Human natural resistance-associated macrophage protein 2: gene cloning and protein identification. *Biochem. Biophys. Res. Commun.* **251**, 775–783
- 29 Garrick, M. D., Gniecko, K., Liu, Y., Cohan, D. S. and Garrick, L. M. (1993) Transferrin and the transferrin cycle in Belgrade rat reticulocytes. *J. Biol. Chem.* **268**, 14867–14874
- 30 Fleming, R. E., Migas, M. C., Zhou, X. Y., Jiang, J. X., Britton, R. S., Brunt, E. M., Tomatsu, S., Waheed, A., Bacon, B. R. and Sly, W. S. (1999) Mechanism of increased iron absorption in murine model of hereditary hemochromatosis: increased duodenal expression of the iron transporter DMT1. *Proc. Natl. Acad. Sci. U.S.A.* **96**, 3143–3148

Received 22 October 1999/14 March 2000; accepted 6 April 2000